Intracellular mRNA Regulation with Self-Assembled Locked Nucleic Acid Polymer Nanoparticles

Anthony M. Rush,[†] David A. Nelles,[§,⊥] Angela P. Blum,[†] Sarah A. Barnhill,[†] Erick T. Tatro,[∥]
Gene W. Yeo,[‡,§] and Nathan C. Gianneschi*,[†,⊥]

[†]Department of Chemistry & Biochemistry, [‡]Stem Cell Program and Institute for Genomic Medicine, [§]Department of Cellular and Molecular Medicine, [∥]Department of Psychiatry, [⊥]Materials Science and Engineering, University of California, San Diego, La Jolla, California 92093, United States

S *Supporting Information*

ABSTRACT: We present an untemplated, single-component antisense oligonucleotide delivery system capable of regulating mRNA abundance in live human cells. While most approaches to nucleic acid delivery rely on secondary carriers and complex multicomponent charge-neutralizing formulations, we demonstrate efficient delivery using a simple locked nucleic acid (LNA)-polymer conjugate that assembles into spherical micellar nanoparticles displaying a dense shell of nucleic acid at the surface. Cellular uptake of soft LNA nanoparticles occurs rapidly within minutes as evidenced by flow cytometry and fluorescence microscopy. Importantly, these LNA nanoparticles knockdown survivin mRNA, an established target for cancer therapy, in a sequence-specific fashion as analyzed by RT-PCR.

Modulation of intracellular RNA abundance provides an exceptional opportunity to study and influence gene function and cellular behavior. In order to systematically exploit this opportunity, the delivery of nucleic acids to relevant biological compartments has been extensively investigated for the past 50 years.[1,2] Despite exhaustive efforts, nucleic acid–based therapies have realized limited success. This shortcoming is largely due to insufficient biostability of nucleic acids, off-target effects of modified nucleic acids, and ultimately the inability to deliver naked nucleic acids across phospholipid membranes.[3,4] The success of nucleic acid-based therapies relies on the ability to rationally design well-defined and stable materials capable of overcoming these barriers. Multicomponent, vector-facilitated nucleic acid delivery has emerged as a powerful tool in the past decade due to convenience, effectiveness, and the ability to adapt materials for *in vivo* experimentation.[5−7] However, progress in multicomponent nucleic acid delivery using viral vectors, lipoplex formulations, or cationic transfection agents has been hindered by numerous setbacks including toxicity, immunogenicity, DNA release, and nucleic acid instability.[8,9] More recently, single-component nucleic acid based materials have been developed as well-defined alternatives to multicomponent DNA delivery systems.[10−13] Spherical nucleic acids (SNAs)[14] represent a unique class of stable[15] DNA delivery vehicles that display nucleic acids at the surface of the nanomaterial, hence eliminating the need to release nucleic acids from a condensed or sequestered state. Materials capable of regulating mRNA

abundance *in cellulo* without the need for the incorporation of a cellular internalizing component have only been demonstrated using metal-templated SNAs.[16,17] Despite the success of gold-core SNAs, the requirement for metal templation imposes certain constraints and limitations on the resulting SNAs including oligo attachment chemistry, chemical diversity of the core itself, and maximum nucleic acid density achievable in the nanoparticle shell.[18] Furthermore, in order to avoid toxicity associated with gold nanoparticle accumulation,[19,20] the template must be chemically dissolved once the material has been synthesized.[21] In the interest of developing multifunctional and nontoxic oligonucleotide delivery agents with novel properties, it is necessary to develop new strategies toward accessing and expanding upon this unique class of materials. In this work we demonstrate that efficient cellular uptake and potent mRNA regulation can be achieved with a new class of spherical nucleic acid, namely LNA-polymer amphiphile (LPA) nanoparticles.

LPA nanoparticles are discrete assemblies of a well-defined polymer-LNA conjugate prepared via solid-phase coupling of a carboxylic acid terminated norbornyl polymer with an amine-modified LNA oligonucleotide on controlled pore glass (CPG) beads. After conjugation, LPAs are cleaved from the solid support with an aqueous base to yield well-defined spherical polymeric micellar nanoparticles (Figure 1). LPA nanoparticle formation in aqueous solution is driven by the hydrophobic effect,[22] hence the micelles are composed of a hydrophobic polynorbornyl core with each polymer covalently bound through an amide linkage to one solvated hydrophilic oligonucleotide in the shell. This chemistry is important in that it drives the dense packing of negatively charged, self-repulsive nucleic acids in the micelle corona via energetically favorable solvent exclusion governed by the hydrophobic polymer core. It is noteworthy to mention that nucleic acid density achieved in the nanoparticle shell is exceptionally high as evidenced in previous work from our laboratory demonstrating that analogous DNA-based nanoparticles can render DNA resistant to degradation by both endo- and exonucleases.[23] LPA nanoparticles average 20 nm in diameter as evidenced by transmission electron microscopy (TEM) and dynamic light scattering (DLS; see Figure 1 and Supporting Information Figures S1−S3). These materials are the first example of a
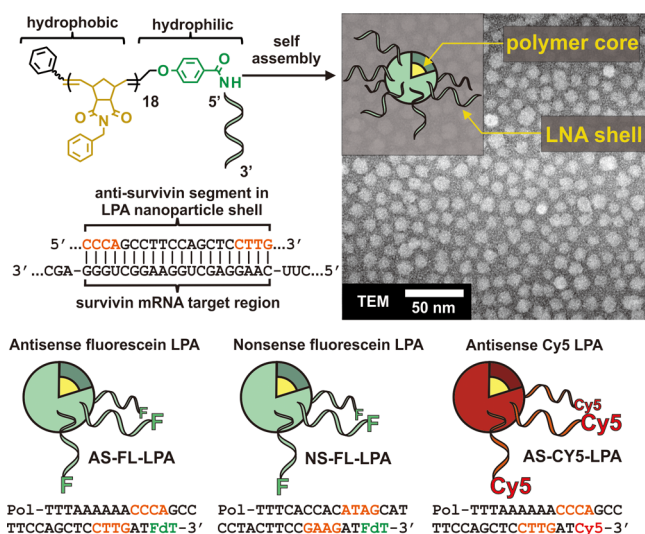
Figure 1. LPA composition and charcterization by electron microscopy. LPAs assemble into spherical micellar nanoparticles as they are released from solid support and dispersed into aqueous solution. The resulting nanoparticles are roughly 20 nm in diameter as evidenced by negative stain TEM and DLS. LPA nanoparticles consist of a hydrophobic polynorbornyl core and a fluorescently labeled hydrophilic LNA shell designed to be complementary (antisense) or noncomplementary (nonsense) to a 20-base region of mRNA responsible for synthesizing the protein survivin. LNA bases are indicated in orange, "Pol" indicates the norbornene polymer conjugated to the 5′ end of the LNA sequence, F and FdT represent fluorescein-modified thymidine, and Cy5 represents an incorporated cyanine 5 phosphoramidite.

Figure 2. Uptake of dye-labeled LPA nanoparticles in HeLa cells. (A) FACS distributions showing the intensity of fluorescence among HeLa cells treated with the antisense fluorescein-labeled LNA-polymer amphiphile (AS-FL-LPA) after a 2 h incubation in the presence of nanoparticles. Data are gated on 2500 total events, λ_{ex} = 488 nm, λ_{em} = 533 ± 15 nm; see Supporting Information Figure S5 for details. (B) FACS data showing fluorescent cell population due to antisense Cy5-labeled (AS-CY5-LPA) micelle uptake in HeLa cells after incubation for 2 h. Data are gated on 2500 total events, λ_{ex} = 640 nm, λ_{em} = 675 ± 12.5 nm; see Supporting Information Figure S6 for details. (C−E) Confocal fluorescence microscopy of AS-FL-LPA-treated HeLa cells (C, λ_{ex} = 488 nm), untreated HeLa cells (D, λ_{ex}= 488 nm, 635 nm), and antisense Cy5 LPA nanoparticle-treated HeLa cells (E, λ_{ex} = 635 nm) showing material uptake and distribution in a single z-slice. Time points are indicated on each panel; scale bars are 50 μm. See Supporting Information Figures S7 and S8 for z-stack images.

nontemplated and purely organic single-component nanoparticle to demonstrate efficient cellular uptake and subsequent mRNA regulation via antisense activity in live cells.

To examine the efficiency of LPA nanoparticle cellular uptake and subsequent interaction with intracellular mRNA, three different LPA nanoparticles were designed and synthesized (Figure 1 and Supporting Information Figure S4). The first micelle, termed antisense fluorescein-labeled LPA (**AS-FL-LPA**) nanoparticle, contains a fluorescently labeled LNA sequence complementary to a 20-base region located in the second exon of survivin mRNA in HeLa cells. As a control, a second micelle was synthesized, termed nonsense fluorescein-labeled LPA (**NS-FL-LPA**) nanoparticle, in which the nucleotide sequence was scrambled. We anticipated that comparison of the activity of these two distinct materials would facilitate determination of the sequence-specific nature of LPA nanoparticle mediated survivin mRNA regulation. A third micelle, termed antisense cyanine 5-labeled LPA (**AS-CY5-LPA**) nanoparticle, was designed to interrogate the influence of the incorporated dye on LPA nanoparticle uptake in HeLa cells.[24−26]

As an initial experiment, **AS-FL-LPA** nanoparticles and the corresponding naked single-stranded fluorescein-labeled LNA sequence were incubated with HeLa cells to investigate the extent of uptake of each species measured by fluorescence-activated cell sorting (FACS, Figure 2). After incubation with 5 nM **AS-FL-LPA** nanoparticle or 1 μM (the equivalent concentration with respect to LNA and fluorescein dye) naked fluorescein-labeled ssLNA analogue for 2 h, FACS analysis reveals an approximately 10-fold increase in population-wide fluorescence at 533 nm for those cells treated with
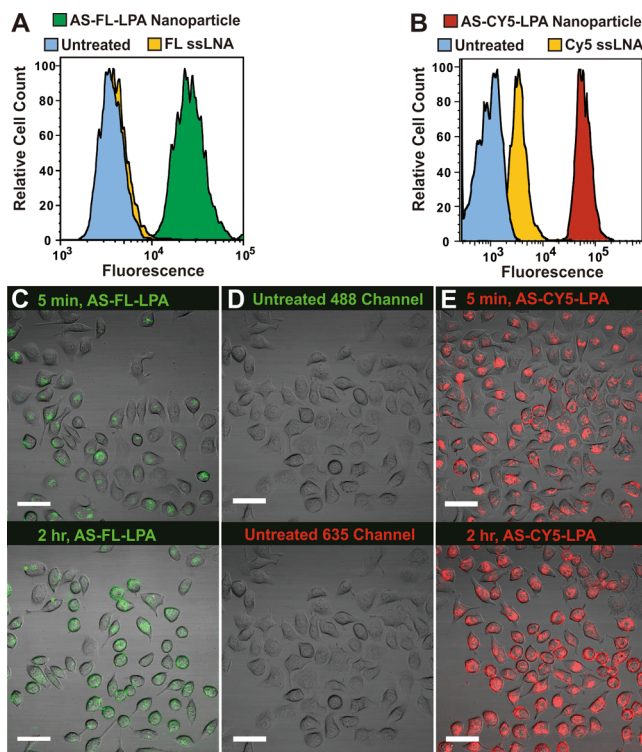
LPA nanoparticles as compared to those treated with the ssLNA analogue (Figure 2A and Supporting Information Figure S5). Uptake for Cy5-labeled LPA nanoparticles shows a similar trend (Figure 2B and Supporting Information Figure S6). However, in contrast to fluorescein-labeled ssLNA, there is observable association of the naked Cy5-labeled ssLNA analogue with HeLa cells. As the LNA nucleobase sequence is identical to that of the fluorescein-labeled ssLNA, this effect may be a result of cyanine 5 incorporation, as certain dye molecules are known to associate with cell membranes.[24−26] Nevertheless, HeLa cells incubated with 5 nM **AS-CY5-LPA** nanoparticles demonstrate a ca. 10-fold increase in fluorescence per cell at 675 nm as compared to those cells treated with the Cy5-labeled ssLNA analogue. These results underscore the importance of the three-dimensional arrangement of oligonucleotides in facilitating cellular association.[14] Indeed, it has been recently demonstrated that other varieties of nanostructured DNA-based materials undergo cellular uptake more efficiently than single-stranded analogues.[27,28]

Having established that LPA nanoparticles associate with HeLa cells by FACS, we performed live-cell z-stack confocal

fluorescence microscopy to determine the extent of nano-particle internalization as well as intracellular distribution (Figure 2 C−E and Supporting Information Figures S7 and S8). Live HeLa cells were imaged after LPA nanoparticle incubation in order to discern the distribution of LPA nanoparticles relative to cellular boundaries without the introduction of artifacts associated with cell fixation. Based on confocal fluorescence images it is apparent that LPA nano-particles are distributed diffusely throughout the cell body in some cells (ca. 70% of cells, as determined by visual inspection of the imaged area) after 10 min of incubation and in almost all imaged cells (ca. 98% of cells, as determined by visual inspection of the imaged area) after 2 h of incubation with LPA nanoparticles. This, along with FACS data, suggests that micelles are rapidly taken up into HeLa cells and effectively distributed in the cytosol.

RNA plays a central role in regulating and propagating genetic information; hence numerous efforts have demon-strated the utility of manipulating the expression of disease-causing genes via interference with various RNAs.[29] To determine if LPA nanoparticles are able to modulate intra-cellular mRNA levels, we designed nanoparticles capable of base-pairing in an antisense fashion specifically with a 20-base region of survivin mRNA, an RNA associated with proliferation of HeLa and other cancerous cells.[30] After treatment with antisense (**AS-FL-LPA**) or nonsense (**NS-FL-LPA**) micelles, total HeLa RNA was harvested and analyzed for relative abundance of survivin mRNA (Figure 3B). Treatment with
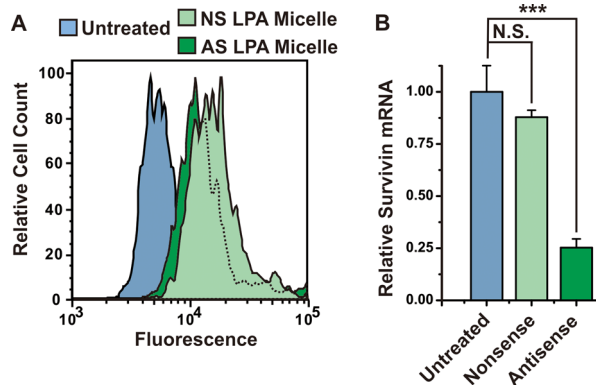

Figure 3. LPA nanoparticle uptake and survivin mRNA depletion. (A) FACS data showing similar uptake for both antisense and nonsense LPA nanoparticles after incubation with HeLa cells for 2 h. λ_{ex}= 488 nm, λ_{em} = 533 ± 15 nm; see Suporting Information Figure S9 for more details. (B) RT-PCR results showing sequence-selective survivin mRNA knockdown due to treatment with antisense LPA nanoparticles (AS-FL-LPA). See Supporting Information Tables S1 and S2 for more information.

antisense LPA nanoparticles significantly depleted survivin mRNA levels relative to endogenous GAPDH mRNA tran-scripts, suggesting efficient, sequence-specific regulation of mRNA levels (Figure 3B). Treatment with nonsense LPA nanoparticles showed no significant effect on survivin mRNA levels when compared to levels in untreated cells. To our knowledge, other than gold-templated SNAs, there has been only one other example in the literature of a DNA-based nanomaterial demonstrating gene-specific interactions without the need for an auxiliary uptake-enhancing component.[31]

Given that cellular uptake and internalization of LPA nanoparticles appears to be rapid and efficient, we investigated

the kinetics, cytotoxicity, and potential mechanism for LPA nanoparticle uptake (Figure 4). Previous reports concerning
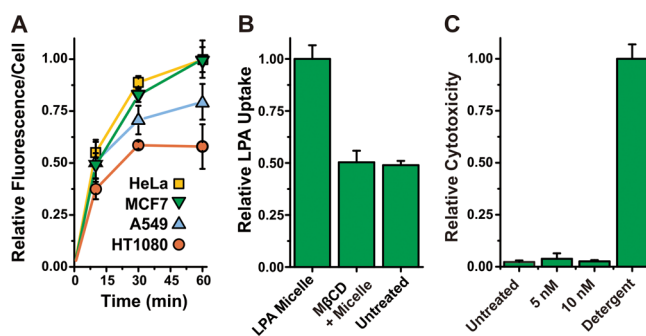

Figure 4. AS-FL-LPA Nanoparticle uptake kinetics, dependence on cholesterol, and cytotoxicity. (A) Compiled FACS data showing LPA nanoparticle uptake over time in various cell lines. Data are gated on a minumum of 2500 events, λ_{ex} = 488 nm, λ_{em} = 533 ± 15 nm; see Supporting Information Figures S10 and S11 for more information. (B) Compiled FACS data showing a decrease in LPA nanoparticle uptake after HeLa cells were treated with methyl-β-cyclodextrin λ_{ex}= 488 nm, λ_{em} = 533 ± 15 nm; see Supporting Information Figures S13, S14, and Tables S4 and S5 for more information. (C) Compiled FACS data showing relative cytotoxicity for 5 nM and 10 nM LPA nanoparticle treatments versus treatment with 0.25% Triton-X 100. Cytotoxicity was assessed via cell-associated propidium iodide fluorescence, λ_{ex} = 488 nm, λ_{em} filter = 670 nm LP. See Supporting Information Figure S15 and Table S6 for more information.

spherical nucleic acids indicate rapid cellular internalization that is dependent on Type A scavenger receptors and cholesterol-dependent caveolae-mediated endocytosis.[32] LPA nanoparticles exhibit rapid uptake within 10 min of introduction to adherent cells across five different cell lines including human embryonic kidney cells (Figure 4A and Supporting Information Figures S10−12, Table S3). LPA nanoparticle association with the cell appears to reach a maximum between 30 and 60 min after incubation for each of the four cancerous cell lines studied. Furthermore, LPA nanoparticle uptake in HeLa cells appears to be dependent on cholesterol, as treatment with methyl-β-cyclodextrin significantly decreases association of LPA nano-particles (Figure 4B). In our hands, treatment with other pharmacological inhibitors or disruptors of the aforementioned endocytotic pathways did not have a significant effect on cellular association in HeLa cells (Supporting Information Figures S13, S14 and Tables S4 and S5). Futhermore, LPA nanoparticles show no appreciable cytotoxicity in HeLa cells when analyzing membrane integrity after 1 h of incubation using propidium iodide as a probe (Figure 4C and Supporting Information Figure S15 and Table S6).

The development of hybrid nucleic acid-based materials capable of facilitating potent and specific interactions in complex biological milieu hinges upon the ability to create well-defined elements with predictable attributes and diverse composition. The straightforward synthesis, high-density dis-play of covalently bound nucleic acids, and the potential for chemical diversification make LPA nanoparticles ideal candi-dates in forming the basis of next generation smart biomaterials capable of recognizing and responding to particular gene expression features.

■ ASSOCIATED CONTENT

S Supporting Information

Detailed materials and sample preparation are included together with additional data and images. This material is available free of charge via the Internet at http://pubs.acs.org.

■ AUTHOR INFORMATION

Corresponding Author

ngianneschi@ucsd.edu.

Notes

The authors declare no competing financial interest.

■ ACKNOWLEDGMENTS

■ REFERENCES

(1) Crawford, L.; Dulbecco, R.; Fried, M.; Montagnier, L.; Stoker, M. *Proc. Natl. Acad. Sci. U.S.A.* **1964**, *52*, 148−152.

(2) Jackson, D. A.; Berg, P.; Symons, R. H. *Proc. Natl. Acad. Sci. U.S.A.* **1972**, *69*, 2904−2909.

(3) Ledley, F. D. *Hum. Gene Ther.* **1995**, *6*, 1129−1144.

(4) Davis, M. E. *Curr. Opin. Biotechnol.* **2002**, *13*, 128−131.

(5) Wu, Z. J.; Asokan, A.; Samulski, R. J. *Mol. Ther.* **2006**, *14*, 316−327.

(6) Luo, D.; Saltzman, W. M. *Nat. Biotechnol.* **2000**, *18*, 33−37.

(7) Kanasty, R.; Dorkin, J. R.; Vegas, A.; Anderson, D. *Nat. Mater.* **2013**, *12*, 967−977.

(8) Crystal, R. G. *Science* **1995**, *270*, 404−410.

(9) Tripathy, S. K.; Black, H. B.; Goldwasser, E.; Leiden, J. M. *Nat. Med.* **1996**, *2*, 545−550.

(10) Meade, B. R.; Dowdy, S. F. *Discovery Med.* **2009**, *8*, 253−256.

(11) Zheng, D.; Giljohann, D. A.; Chen, D. L.; Massich, M. D.; Wang, X. Q.; Iordanov, H.; Mirkin, C. A.; Paller, A. S. *Proc. Natl. Acad. Sci. U.S.A.* **2012**, *109*, 11975−11980.

(12) Jensen, S. A.; Day, E. S.; Ko, C. H.; Hurley, L. A.; Luciano, J. P.; Kouri, F. M.; Merkel, T. J.; Luthi, A. J.; Patel, P. C.; Cutler, J. I.; Daniel, W. L.; Scott, A. W.; Rotz, M. W.; Meade, T. J.; Giljohann, D. A.; Mirkin, C. A.; Stegh, A. H. *Science Trans. Med.* **2013**, *5*, 209ra152.

(13) Averick, S. E.; Paredes, E.; Dey, S. K.; Snyder, K. M.; Tapinos, N.; Matyjaszewski, K.; Das, S. R. *J. Am. Chem. Soc.* **2013**, *135*, 12508−12511.

(14) Cutler, J. I.; Auyeung, E.; Mirkin, C. A. *J. Am. Chem. Soc.* **2012**, *134*, 1376−1391.

(15) Seferos, D. S.; Prigodich, A. E.; Giljohann, D. A.; Patel, P. C.; Mirkin, C. A. *Nano Lett.* **2009**, *9*, 308−311.

(16) Rosi, N. L.; Giljohann, D. A.; Thaxton, C. S.; Lytton-Jean, A. K. R.; Han, M. S.; Mirkin, C. A. *Science* **2006**, *312*, 1027−1030.

(17) Prigodich, A. E.; Seferos, D. S.; Massich, M. D.; Giljohann, D. A.; Lane, B. C.; Mirkin, C. A. *ACS Nano* **2009**, *3*, 2147−2152.

(18) Hurst, S. J.; Lytton-Jean, A. K. R.; Mirkin, C. A. *Anal. Chem.* **2006**, *78*, 8313−8318.

(19) Alkilany, A. M.; Murphy, C. J. *J. Nanopart. Res.* **2010**, *12*, 2313−2333.

(20) Chompoosor, A.; Saha, K.; Ghosh, P. S.; Macarthy, D. J.; Miranda, O. R.; Zhu, Z. J.; Arcaro, K. F.; Rotello, V. M. *Small* **2010**, *6*, 2246−2249.

(21) Young, K. L.; Scott, A. W.; Hao, L. L.; Mirkin, S. E.; Liu, G. L.; Mirkin, C. A. *Nano Lett.* **2012**, *12*, 3867−3871.

(22) Tanford, C. *Proc. Natl. Acad. Sci. U.S.A.* **1979**, *76*, 4175−4176.

(23) Rush, A. M.; Thompson, M. P.; Tatro, E. T.; Gianneschi, N. C. *ACS Nano* **2013**, *7*, 1379−1387.

(24) Rubalcav, B.; Demunoz, D. M.; Gitler, C. *Biochemistry* **1969**, *8*, 2742−2747.

(25) Sims, P. J.; Waggoner, A. S.; Wang, C. H.; Hoffman, J. F. *Biochemistry* **1974**, *13*, 3315−3330.

(26) Johnson, L. V.; Walsh, M. L.; Chen, L. B. *Proc. Natl. Acad. Sci. U.S.A.* **1980**, *77*, 990−994.

(27) Alemdaroglu, F. E.; Alemdaroglu, N. C.; Langguth, P.; Herrmann, A. *Macromol. Rapid Commun.* **2008**, *29*, 326−329.

(28) Hamblin, G. D.; Carneiro, K. M. M.; Fakhoury, J. F.; Bujold, K. E.; Sleiman, H. F. *J. Am. Chem. Soc.* **2012**, *134*, 2888−2891.

(29) Hannon, G. J. *Nature* **2002**, *418*, 244−251.

(30) Ambrosini, G.; Adida, C.; Altieri, D. C. *Nat. Med.* **1997**, *3*, 917−921.

(31) Chen, T.; Wu, C. S.; Jimenez, E.; Zhu, Z.; Dajac, J. G.; You, M. X.; Han, D.; Zhang, X. B.; Tan, W. H. *Angew. Chem., Int. Ed.* **2013**, *52*, 2012−2016.

(32) Choi, C. H. J.; Hao, L. L.; Narayan, S. P.; Auyeung, E.; Mirkin, C. A. *Proc. Natl. Acad. Sci. U.S.A.* **2013**, *110*, 7625−7630.